Radionuclide Imaging of Osteomyelitis

Christopher J. Palestro, MD[*,†]

Radionuclide procedures frequently are performed as part of the diagnostic workup of osteomyelitis. Bone scintigraphy accurately diagnoses osteomyelitis in bones not affected by underlying conditions. Degenerative joint disease, fracture, and orthopedic hardware decrease the specificity of the bone scan, making it less useful in these situations. Gallium-67 scintigraphy was often used as an adjunct to bone scintigraphy for diagnosing osteomyelitis. However, now it is used primarily for spinal infections when ^{18}F-FDG imaging cannot be performed. Except for the spine, in vitro–labeled leukocyte imaging is the nuclear medicine test of choice for diagnosing complicating osteomyelitis. Leukocytes accumulate in bone marrow as well as in infection. Performing complementary bone marrow imaging with ^{99m}Tc-sulfur colloid facilitates the differentiation between osteomyelitis and normal marrow and improves test overall accuracy. Antigranulocyte antibodies and antibody fragments, such as ^{99m}Tc-besilesomab and ^{99m}Tc-sulesomab, were developed to eliminate the disadvantages associated with in vitro–labeled leukocytes. These agents, however, have their own shortcomings and are not widely available. As biotin is used as a growth factor by certain bacteria, ^{111}In-biotin is useful to diagnose spinal infections. Radiolabeled synthetic fragments of ubiquicidin, a naturally occurring human antimicrobial peptide that targets bacteria, can differentiate infection from sterile inflammation and may be useful to monitor response to treatment. ^{18}F-FDG is extremely useful in the diagnostic workup of osteomyelitis. Sensitivity in excess of 95% and specificity ranging from 75%-99% have been reported. ^{18}F-FDG is the radionuclide test of choice for spinal infection. The test is sensitive, with a high negative predictive value, and reliably differentiates degenerative from infectious vertebral body end-plate abnormalities. Data on the accuracy of ^{18}F-FDG for diagnosing diabetic pedal osteomyelitis are contradictory, and its role for this indication remains to be determined. Initial investigations suggested that ^{18}F-FDG accurately diagnoses prosthetic joint infection; more recent data indicate that it cannot differentiate infection from other causes of prosthetic failure. Preliminary data on the PET agents gallium-68 and iodine-124 fialuridine indicate that these agents may have a role in diagnosing osteomyelitis.
Semin Nucl Med 45:32-46 © 2015 Elsevier Inc. All rights reserved.

Osteomyelitis is an infection of the bone and may be localized or involve periosteum, cortex, marrow, and cancellous tissue. Acute osteomyelitis can arise hematogenously or through inoculation from direct trauma, a contiguous focus of infection, or sepsis following surgery.[1] The diagnosis of osteomyelitis is not always obvious, and radionuclide procedures frequently are performed as part of the diagnostic workup.

*Department of Radiology Hofstra, NorthShore-LIJ School of Medicine, Hempstead, NY.
†Division of Nuclear Medicine and Molecular Imaging, North Shore Long Island Jewish Health System, Manhasset & New Hyde Park, NY.
Address reprint requests to Christopher J. Palestro, MD, Division of Nuclear Medicine and Molecular Imaging, Long Island Jewish Medical Center, 270-05 76th Ave, New Hyde Park, NY 11040. E-mail: palestro@lij.edu

Radiopharmaceuticals

Single-Photon–Emitting Agents

[99m]Tc-Diphosphonates

Bone scintigraphy usually is performed with technetium-99m-methylene diphosphonate (^{99m}Tc-MDP). Uptake of this radiopharmaceutical, which binds to the hydroxyapatite crystal, depends on blood flow and rate of new bone formation. When osteomyelitis is the indication, a 3-phase bone scan usually is performed. Three-phase bone scintigraphy consists of a dynamic imaging sequence, the flow or perfusion phase, followed immediately by static images of the region of interest, the blood pool or soft tissue phase. The third, or bone, phase consists of images of the area of interest, acquired 2-4 hours after injection. Focal hyperperfusion, focal hyperemia, and focally increased

Flow   Blood Pool   Bone

Figure 1 Right ulnar osteomyelitis. There is focal hyperperfusion, focal hyperemia, and focally increased bone uptake of radiopharmaceutical in the right ulna.

bony uptake are the classic presentation of osteomyelitis on a 3-phase bone scan (Fig. 1). The test is both sensitive and specific for diagnosing osteomyelitis in bones not affected by underlying conditions. Abnormalities on bone scintigraphy reflect the rate of new bone formation in general and consequently in the setting of preexisting conditions such as degenerative joint disease, fracture, and orthopedic hardware, the test, because of decreased specificity, is less useful (Fig. 2).[2]

Gallium-67

Several factors contribute to gallium-67 (^{67}Ga) uptake in infection. Approximately 90% of circulating ^{67}Ga is transferrin bound in the plasma. Increased blood flow and vascular membrane permeability result in increased ^{67}Ga delivery and accumulation at infectious foci. ^{67}Ga binds to lactoferrin, which is present in high concentrations in sites of infection. Direct bacterial uptake, complexing with siderophores, and leukocyte transport also may contribute to ^{67}Ga uptake in infection. Imaging generally is performed 18-72 hours after injection.[2] Presently, the role of ^{67}Ga imaging in musculoskeletal infection is limited almost exclusively to the spine (Fig. 3).

In Vitro–Labeled Leukocytes

In vitro leukocyte (white blood cell [WBC]) labeling usually is performed with ^{111}In oxyquinolone (In) or

^{99m}Tc-exametazime (Tc). Uptake depends on intact chemotaxis, number and types of cells labeled, and cellular response in a particular condition. A circulating WBC count of at least 2000 per microliter is needed for satisfactory image quality. Most WBCs labeled usually are neutrophils, and the test is most sensitive for detecting neutrophil-mediated infections.[3]

^{111}In-WBC advantages include label stability; a normal distribution limited to liver, spleen, and bone marrow; and the ability to perform delayed imaging. Complementary bone marrow imaging can be performed during cell labeling, as a simultaneous dual-isotope acquisition, or after ^{111}In-WBC imaging. Disadvantages include low-resolution images and the interval of 16-30 hours between injection and imaging.[3]

The normal distribution of ^{99m}Tc-WBCs is more variable than that of ^{111}In-WBCs. In addition to the reticuloendothelial system, activity normally is present in the urinary tract, large bowel (within 4 hours after injection), and occasionally gall bladder. ^{99m}Tc-WBC advantages include high-resolution images, and the ability to detect abnormalities within a few hours after injection. Disadvantages include label instability and the short half-life of ^{99m}Tc, which limits delayed imaging. When performing bone marrow imaging, there must be an interval of 2-3 days between the 2 procedures.[3]

Leukocytes accumulate in both infection and bone marrow. The normal distribution of hematopoietically active bone

Flow   Blood Pool   Bone
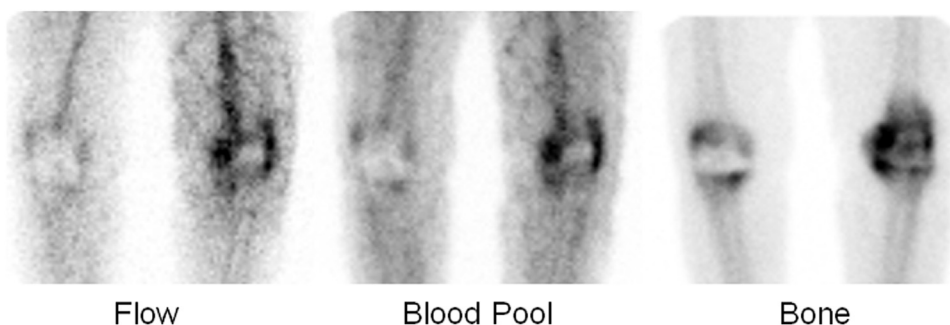
Figure 2 Left knee osteoarthritis. The findings on the 3-phase bone scan in this case mimic those seen in osteomyelitis, illustrating the limitations of bone scintigraphy in individuals with preexisting skeletal abnormalities. This study was performed to evaluate a painful right knee arthroplasty; the left knee was asymptomatic.
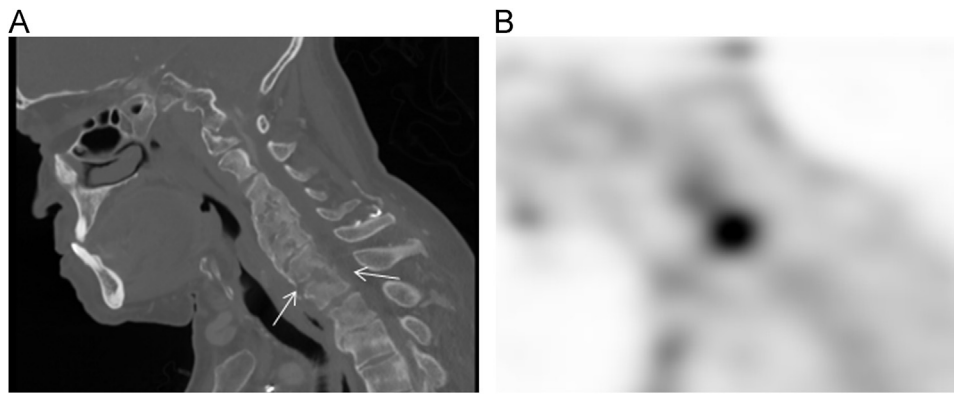
Figure 3 Cervical spine osteomyelitis. The sagittal CT image (left) demonstrates destructive changes at the C6-C7 level (arrows), which corresponds to an area of intense radiopharmaceutical uptake on the sagittal ^{67}Ga SPECT image (right).

marrow is variable and is affected by the patient's age, systemic conditions such as sickle cell disease and tumor, and local conditions such as fractures and orthopedic hardware. Consequently, it may not be possible to determine if an area of activity on a WBC image represents infection or marrow. Performing ^{99m}Tc-sulfur colloid bone marrow (marrow) imaging overcomes this difficulty. Both WBCs and ^{99m}Tc-sulfur colloid accumulate in marrow; WBCs also accumulate in infection, but sulfur colloid does not. The combined study result is positive for infection when activity is present on the WBC image without corresponding activity on the marrow image. Any other pattern is negative for infection (Figs. 4 and 5).[4]

In Vivo–Labeled Leukocytes

Besilesomab, a 150-kDa murine monoclonal antibody of the IgG1 kappa isotype, binds to nonspecific cross-reacting antigen-95, an epitope expressed on cell membranes of granulocytes and granulocyte precursors. Approximately 10% of the ^{99m}Tc-besilesomab injected is neutrophil bound by 45 minutes. Another 20% circulates freely, presumably localizing in infection through nonspecific mechanisms. The incidence of human antimurine antibody response ranges from

less than 5% in patients receiving a single dose of 125 μg of antibody to more than 30% in patients receiving repeated injections. To minimize potential problems, patients should be prescreened for human antimurine antibody, injected with no more than 250 μg of antibody, and should avoid repeat administration.[5]

Sulesomab, a 50-kDa fragment antigen-binding (Fab′) portion of an IgG1 class murine monoclonal antibody, binds to normal cross-reactive antigen-90 present on leukocytes. Approximately 3%-6% of the ^{99m}Tc-sulesomab injected is associated with circulating neutrophils; at 24 hours after injection, approximately 35% of the remaining activity is in the bone marrow. Initial investigations suggested that sulesomab binds to circulating neutrophils that migrate to foci of infection and to leukocytes already present at the site of infection. Subsequent data, however, suggest that accumulation in infection is nonspecific.[5]

[111]In-Biotin

Biotin is necessary for cell growth, fatty acid production, and metabolism of fats and amino acids. It also is used as a growth factor by certain bacteria. ^{111}In-biotin has been used primarily for diagnosing spinal infections.[5]

^{111}In-WBC   ^{99m}Tc-Sulfur Colloid
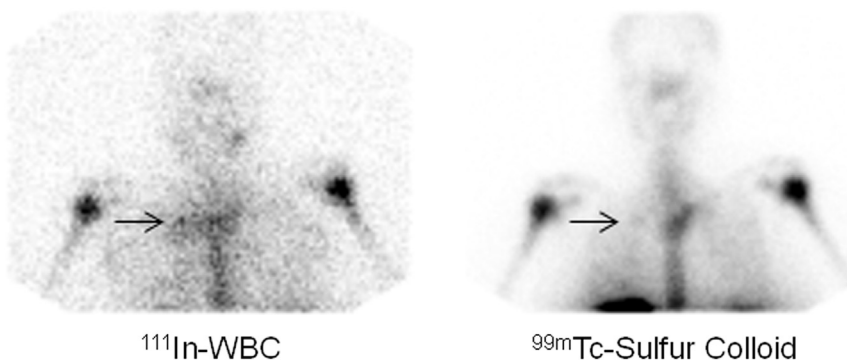
Figure 4 Right sternoclavicular osteomyelitis. Noncontrast CT scan finding (not shown), in a patient with right anterior chest wall mass, swelling, and tenderness, was interpreted as consistent with myositis adjacent to the medial head of the right clavicle and in the right retrosternal region. On the ^{111}In-WBC image (left), the right sternoclavicular region (arrow) appears slightly larger than the left. The intensity of the uptake, however, is virtually the same, making it difficult to draw any conclusions. On the marrow image (right), there is a well-defined photopenic defect (arrow) in the medial head of the right clavicle extending into the right half of the manubrium. The combined study result is positive for osteomyelitis.

^{111}In-WBC ^{99m}Tc-Sulfur Colloid
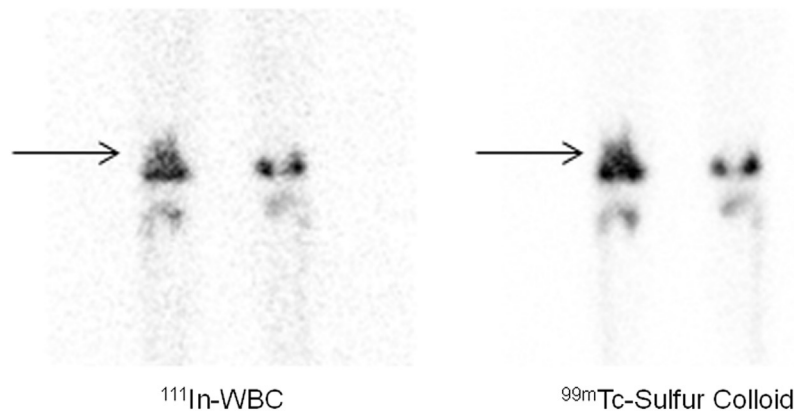
Figure 5 Marrow expansion. Interpreted in isolation, the intense activity in the distal right femur (arrow) on the ^{111}In-WBC image (left) could easily be mistaken for osteomyelitis. On the marrow image (right), the distribution of activity in the distal right femur (arrow) is virtually identical to that on the ^{111}In-WBC image, and the combined study finding is negative for osteomyelitis. The intensity of uptake on labeled leukocyte images is not useful for determining the presence or absence of osteomyelitis. (Compare with Fig. 4).

Radiolabeled Antimicrobial Peptides

Antimicrobial peptides are an integral component of the biological defenses of multicellular organisms. Radiolabeled synthetic fragments of ubiquicidin (UBI), a human antimicrobial peptide that targets bacteria, possess the ability to differentiate infection from sterile inflammation and may be useful for monitoring the efficacy of antibacterial agents in certain infections.[5]

Positron-Emitting Agents
^{18}F-FDG

^{18}F-FDG is transported into cells via glucose transporters and phosphorylated by hexokinase to ^{18}F-2′-^{18}F-FDG-6 phosphate but is not metabolized further. ^{18}F-FDG accumulates in virtually all leukocytes, and its uptake in these cells is related to their metabolic rate and the number of glucose transporters. Increased ^{18}F-FDG accumulation in infection presumably is due to several factors. There is an increased number of glucose transporters and an increased expression of these glucose transporters by activated inflammatory cells. There is an increased affinity of these transporters for ^{18}F-FDG in inflammation, probably owing to the effects of circulating cytokines and growth factors.[6]

^{18}F-FDG PET offers several advantages over single-photon–emitting tracers. PET is a high-resolution tomographic technique that enables precise localization of radiopharmaceutical accumulation. The small ^{18}F-FDG molecule enters poorly perfused areas rapidly. The procedure is completed in 1-2 hours and has a relatively low radiation dose. Uptake usually
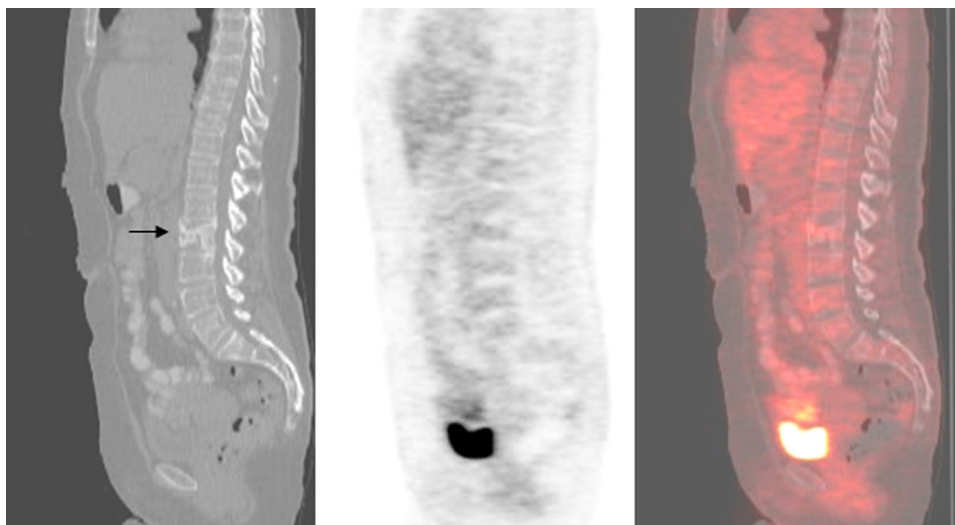
Figure 6 Lumbar spine compression fracture. A 3-month-old compression fracture of the third lumbar vertebra (arrow) can be appreciated on the CT component of the study. There is uniform distribution of ^{18}F-FDG throughout the lumbar spine including the third lumbar vertebra. (Reproduced with permission from Palestro.[6])

normalizes within 3-4 months after trauma or surgery. Degenerative bone changes ordinarily show only mildly increased ^{18}F-FDG uptake (Figs. 6 and 7).[6]

^{18}F-FDG-Labeled Leukocytes

In an effort to develop a more specific PET tracer for infection imaging, leukocytes have been labeled in vitro with ^{18}F-FDG. Despite satisfactory results, it is unlikely that ^{18}F-FDG-WBC imaging ever will enter clinical practice. The 110 minutes half-life of ^{18}F makes it impractical for labeling to be performed off-site, which means that the test would be limited to those sites capable of performing labeling. In some situations, imaging at later time points (eg, 24 hours after injection) may be needed. The short half-life of ^{18}F precludes imaging much later than 4-5 hours after injection. The labeling efficiency is significantly lower and more variable than what can be achieved with ^{111}In-oxine, and, perhaps most importantly, a large fraction of ^{18}F-FDG rapidly elutes from the leukocytes. In vitro data indicate that, by 4 hours after labeling, approximately 40% of the activity is eluted from the cells.[7-11]

Gallium-68

This PET tracer is generator produced. The imaging characteristics of gallium-68 (^{68}Ga) are superior to those of ^{67}Ga. ^{68}Ga has a high positron yield and a half-life of 68 minutes. ^{68}Ga-citrate is produced with high radiochemical yield and purity and has been used to detect inflammation and infection.[5,12]

^{124}I-fialuridne

Bacteria possess a thymidine kinase whose substrate specificity is different from that of the major human thymidine kinase. This difference was used to develop a molecular imaging test for detecting viable bacteria. The potential of ^{124}I-fialuridne

(FIAU) PET/CT for diagnosing musculoskeletal infection was studied in 8 subjects with suspected musculoskeletal infection and 1 control. All patients with musculoskeletal infection demonstrated ^{124}I-FIAU accumulation at the site of infection within 2 hours after injection. There was no abnormal radiopharmaceutical uptake in the 1 control.[5,13]

Indications

It is important to recognize that no single agent is equally efficacious in all regions of the skeleton. The selection of an appropriate study is governed by the clinical question posed. In adults, it is useful to divide musculoskeletal infections into 3 broad locations: spine, orthopedic hardware, and diabetic foot.

Spinal Infection

Spinal osteomyelitis-discitis, which has a predilection for the elderly, accounts for 2%-7% of all cases of osteomyelitis. Infection usually is confined to the vertebral body and intervertebral disc, but the posterior elements are involved in up to 20% of cases. Soft tissue abscesses often accompany spinal infection.[14]

MRI is the best imaging available for spinal infection. Radionuclide imaging is a useful adjunct to MRI. Although bone scintigraphy frequently is used as a screening test, false negative results have been reported in the elderly, possibly secondary to arteriosclerosis-induced ischemia. The test is not useful for detecting soft tissue infections that often accompany, or mimic, spinal osteomyelitis. Abnormalities may persist even after the infection has resolved, owing to ongoing bony remodeling during healing. Consequently, if used at all, bone
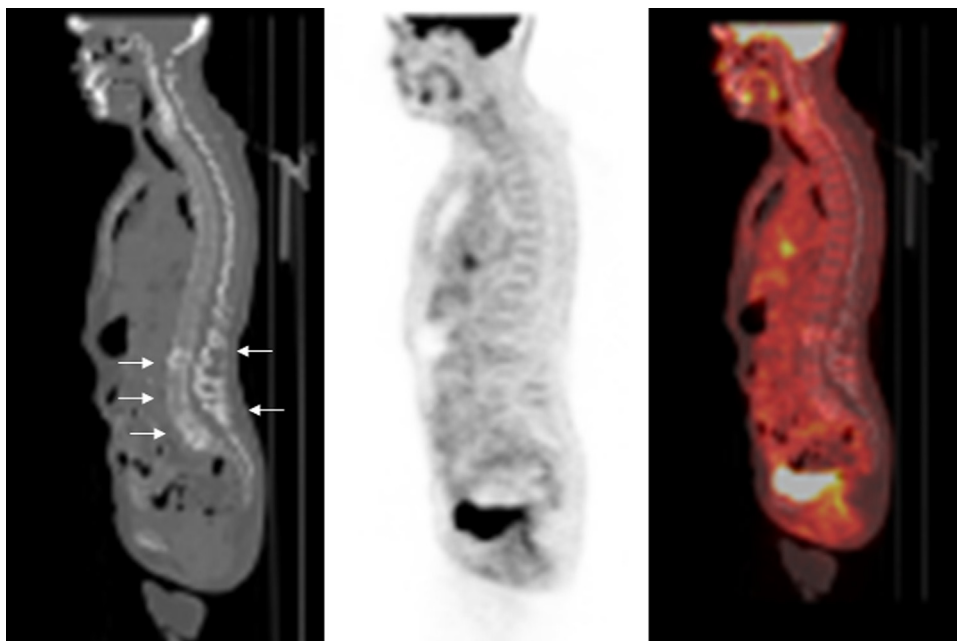
Figure 7 Degenerative spinal arthritis. Although there are extensive degenerative changes (arrows) on the CT component of the examination, there is uniform distribution of ^{18}F-FDG throughout the lumbar spine.

scintigraphy should not be the only radionuclide test performed.[14-16]

Complementary ^{67}Ga imaging improves the specificity of the bone scan. [67]Ga may detect infection sooner than the bone scan and can identify accompanying soft tissue infection. Love et al[14] reported that ^{67}Ga SPECT is as accurate as combined bone-gallium imaging for diagnosing spinal osteomyelitis and concluded that when ^{67}Ga SPECT was performed the bone scan was unnecessary (Fig. 3).

There are few data on the role of ^{67}Ga SPECT-CT in the diagnosis of spinal infection. Lievano et al[17] reported that ^{67}Ga SPECT-CT precisely localized focal radiopharmaceutical uptake seen on planar images, thereby avoiding a false-positive diagnosis of spinal osteomyelitis. Domínguez et al[18] reported that the combination of functional and anatomical images improves disease detection. Fuster et al[19] reported that ^{67}Ga SPECT-CT helped identify soft tissue involvement in 10 of 18 patients with spinal osteomyelitis.

[67]Ga imaging, regardless of how it is performed, has limitations. The physical characteristics and normal biodistribution of the agent are impediments to image analysis. Although the test result may become positive within a few hours, imaging typically is performed 18-72 hours after injection, necessitating multiple visits to nuclear medicine. There is nothing specific about ^{67}Ga uptake in infection; it accumulates in many other conditions, including tumor and trauma.

With all of the limitations inherent in radionuclide bone and ^{67}Ga imaging, it is not surprising that investigators have sought alternative tracers. Lazzeri et al[20] reported that ^{111}In-biotin, alone and in combination with strepavidin, accurately diagnoses spinal infections. ^{111}In-biotin does not accumulate in normal bone or bone marrow and there are few anatomic landmarks on the images. Including SPECT-CT as part of the procedure affects patient management by accurately differentiating bone from soft tissue infection and guiding the selection of therapy.[21]

Published data strongly support the value of ^{18}F-FDG for diagnosing spinal infection.[22-28] Guhlmann et al[22] reported that ^{18}F-FDG-PET correctly diagnosed all 3 cases of infection and was true negative in 1 patient without infection. In another series, Guhlmann et al[23] reported that ^{18}F-FDG-PET was significantly more accurate than ^{99m}Tc-besilesomab for diagnosing spinal osteomyelitis. Schiesser et al[24] reported that in 6 patients with possible spinal implant infection, ^{18}F-FDG-PET finding was true negative for infection in all. In another series, ^{18}F-FDG-PET yielded true-positive results in all 7 patients with spinal osteomyelitis.[25] Schmitz et al[26] reported that the test result was true positive in all 12 patients with spinal infection and true negative in 3 of 4 patients without infection. In a prospective study of 8 patients (9 sites), suspected of having spinal osteomyelitis, Meller et al[27] reported that FDG-PET was 100% accurate.

Hartmann et al,[28] as part of a larger investigation, reported that ^{18}F-FDG-PET-CT finding was true positive in all 7 patients with spinal osteomyelitis and true negative in both patients without spinal osteomyelitis. The precise anatomical localization provided by PET-CT was useful for planning surgical intervention and for differentiating soft tissue from bone involvement, thereby guiding treatment.

Gratz et al[29] observed that ^{18}F-FDG-PET was superior to ^{67}Ga for detecting paraspinal soft tissue infection and was superior to bone scintigraphy for differentiating advanced degenerative arthritis from infection. Fuster et al[19] studied 34 patients, including 18 with spinal osteomyelitis. The sensitivity, specificity, and accuracy of ^{18}F-FDG-PET-CT were 89%, 88%, and 88%, respectively. The sensitivity, specificity, and accuracy of combined bone-gallium imaging were 78%, 81%, and 79%, respectively. ^{18}F-FDG-PET-CT identified soft tissue infection in 12 patients; ^{67}Ga SPECT-CT identified soft tissue involvement in 10 patients.

Gratz et al[29] reported that ^{18}F-FDG-PET was superior to MRI for detecting low-grade spondylitis or discitis. Ohtori et al[30] studied 18 patients with Modic type 1 changes on MRI, including 11 with spinal osteomyelitis who underwent ^{18}F-FDG-PET. The authors reported that there was a 100% concordance between the results of ^{18}F-FDG-PET and the final diagnosis.

Stumpe et al[31] compared ^{18}F-FDG-PET with MRI in 30 patients (38 sites) with lumbar spine vertebral end-plate abnormalities. ^{18}F-FDG-PET finding was true positive in all 5 infected sites and true negative in all 33 uninfected sites (100% sensitivity and 100% specificity). The sensitivity and specificity of MRI were 50% and 96%, respectively (Fig. 8).

Seifen et al[32] analyzed 38 consecutive cases of suspected spondylodiscitis in patients with inconclusive results on MRI or other conventional modalities. A total of 22 patients were diagnosed with spinal osteomyelitis. The sensitivity, specificity, and accuracy of ^{18}F-FDG-PET-CT were 81.8%, 100%, 89.5%, respectively; positive predictive value and negative predictive value were 100% and 80%, respectively. Sensitivity, specificity, and accuracy of MRI, which was performed in 27 cases, were 75%, 71.4%, 74.1%, respectively; the positive predictive value and negative predictive value were 88.2% and 50%, respectively.

There are potential limitations to the test. It is likely that [18]FDG-PET and PET-CT will be less reliable for differentiating infection from tumor and infection superimposed on tumor. ^{18}F-FDG accumulation in degenerative changes usually is relatively low, but significant focal ^{18}F-FDG uptake in degenerative spine disease has been reported.[33]

The presence of a foreign body can incite an intense immune response, and increased ^{18}F-FDG uptake around spinal implants, in the absence of infection, has been observed. de Winter et al[34] reported that the specificity of ^{18}F-FDG-PET was considerably lower in patients with than in patients without spinal implants (65% vs 92%).

Regardless of its potential limitations, the data accumulated over the past several years demonstrate convincingly that ^{18}F-FDG imaging accurately diagnoses spinal osteomyelitis and support its use as an adjunct to MRI. The test is sensitive, completed in a single session, and image quality is superior to that obtained with single-photon–emitting tracers, even when SPECT-CT is performed. Finally, in comparative investigations, ^{18}F-FDG has outperformed bone and ^{67}Ga imaging.
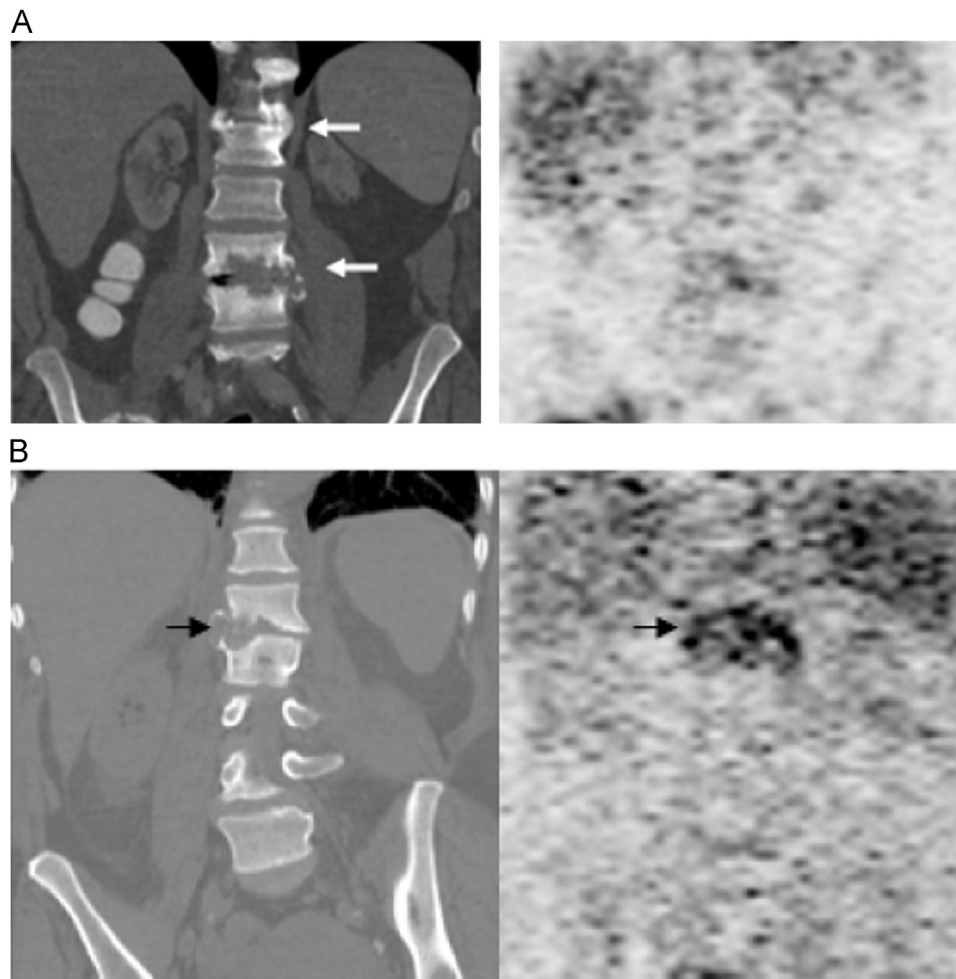
Figure 8 (A) Vertebral end-plate destruction. On the coronal CT image (left), there are degenerative changes (upper arrow) and loss of disc space with destruction of the vertebral end plates at L3-L4 (lower arrow). There is normal ^{18}F-FDG accumulation throughout the lumbar spine on the PET image (right). Bone biopsy and culture findings were negative for infection. (B) Lumbar spine osteomyelitis. On the coronal CT image (left), there is loss of disc space with destruction of the vertebral endplates at L1-L2 (arrow). There is a corresponding area of hypermetabolism (arrow) on the coronal ^{18}F-FDG-PET image (right). ^{18}F-FDG is a useful adjunct to MRI and can facilitate the differentiation between severe degenerative changes and infection. (Reproduced with permission from Palestro.[6])

There are limited data available on the role of ^{68}Ga imaging of spinal infection. Nanni et al[35] reported on 31 patients with suspected osteomyelitis or discitis who underwent ^{68}Ga PET/CT scans. An overall accuracy of 90% was found, and the authors concluded that ^{68}Ga potentially could be useful for this indication.

## Non–Prosthetic Joint Orthopedic Hardware

Combined WBC-marrow imaging has emerged as the imaging test of choice for diagnosing most cases of "complicating" osteomyelitis, including orthopedic hardware infection. The role of ^{18}F-FDG-PET in the evaluation of orthopedic hardware infection has been extensively investigated, and the results have been very satisfactory. Guhlmann et al[22] as part of a larger investigation, reported that ^{18}F-FDG-PET correctly classified the 6 orthopedic implants studied as infected ($n = 5$) or uninfected ($n = 1$). In another investigation, Guhlmann et al[23] reported that ^{18}F-FDG-PET

was comparable to ^{99m}Tc-besilesomab for diagnosing orthopedic implant infection.

De Winter et al[36] investigated ^{18}F-FDG-PET in suspected chronic osteomyelitis, including 17 patients with orthopedic implants. ^{18}F-FDG-PET was true positive in all 10 infected devices (100% sensitivity) and true negative in 6 of 7 uninfected devices (86% specificity).

Schiesser et al[24] prospectively investigated ^{18}F-FDG-PET in posttraumatic orthopedic implant–associated infection in 22 patients. Sensitivity, specificity, and accuracy were 100%, 93%, and 97%, respectively. Retrospective analysis of the results found that the test influenced patient management in nearly two-thirds of the cases.

Hartmann et al[28] investigated ^{18}F-FDG-PET-CT in 33 trauma patients, including 18 with orthopedic implants, 11 of which were infected. The test result was true positive in 10 cases (91% sensitivity) and true negative in 5 cases (71% specificity). Surgeons analyzed the influence of ^{18}F-FDG-PET-CT on patient management and found that

A

Flow   Blood Pool   Bone

B

Flow   Blood Pool   Bone
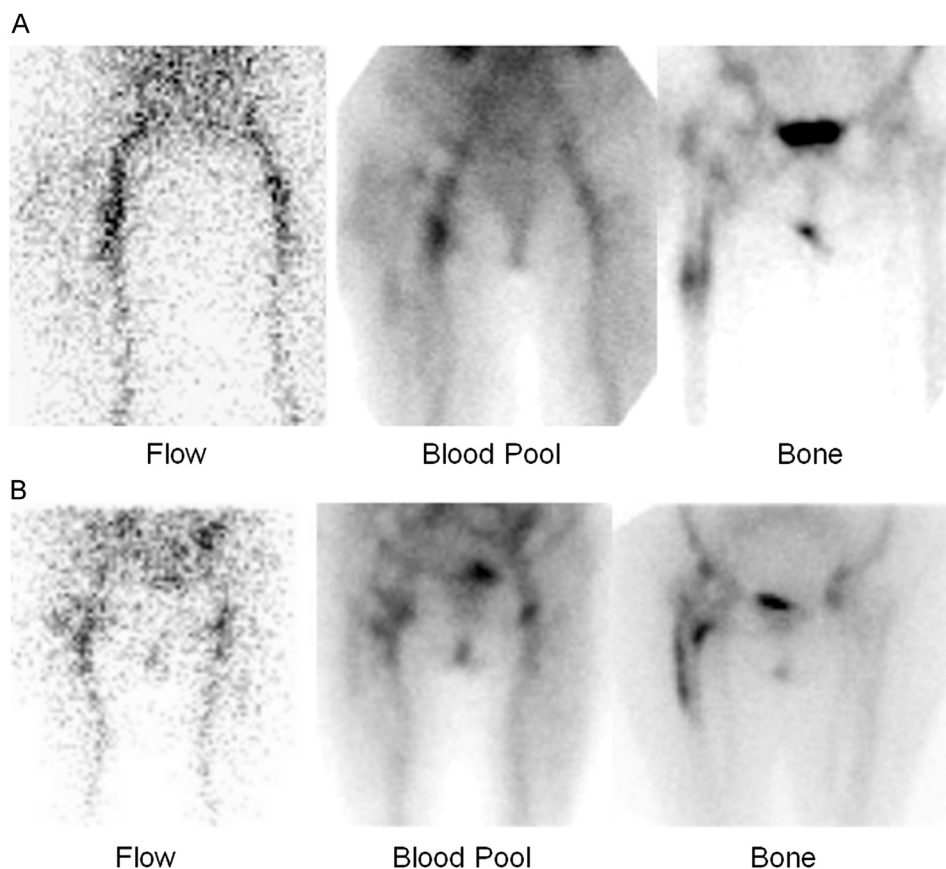
Figure 9 (A) Infected right hip arthroplasty. There is mild hyperperfusion and hyperemia, with irregularly increased radiopharmaceutical accumulation on the bone phase, around the 3-year-old right hip arthroplasty. (B) Aseptically loosened right hip arthroplasty. The findings on this 3-phase bone scan are very similar to those in (A). Most investigators agree that the 3-phase bone scan does not improve accuracy of the test for differentiating infection from other causes of joint replacement failure.

the test contributed relevant information in more than half of the cases.

Prosthetic Joint Infection

Nearly 1 million lower extremity arthroplasties are performed annually in the United States. Aseptic loosening, the most common cause of prosthetic failure, usually is caused by an inflammatory reaction to 1 or more of the prosthetic components. A synovial-like pseudomembrane develops, consisting of histiocytes (95% of specimens), giant cells (80%), and occasionally, lymphocytes and plasma cells (25%). Neutrophils rarely are present (10%).[37] Aseptic loosening usually is managed by a single-stage exchange arthroplasty completed in a single hospital admission with 1 surgical intervention.

Infection accounts for approximately 2% of primary implant failures and approximately 5% of revision implant failures. The inflammatory reaction accompanying the infected prosthesis can be similar to that in aseptic loosening, except that neutrophils, which rarely are present in aseptic loosening, invariably are present, and usually in large numbers.[37] The treatment of the infected joint replacement usually involves more than 1 hospital admission. An excisional arthroplasty is performed followed by weeks to months of antimicrobial therapy, followed eventually by a revision arthroplasty.

Because their management is so very different, distinguishing aseptic loosening from infection of a prosthetic joint is extremely important. A sensitive but nonspecific test can result in multiple unnecessary, and costly, operations when a single intervention would have sufficed. The specific, but insensitive, test also will result in additional surgical interventions, because undiagnosed infection will cause any revision implant to fail with potentially serious consequences.[37]

Joint aspiration with culture is the definitive preoperative diagnostic procedure. Though specific, the sensitivity of this test is variable. Tomas et al[38] reported that joint aspiration with culture was 100% specific but only 70% sensitive for diagnosing prosthetic hip infection.

Among imaging studies, radiographs are not specific and hardware-induced artifacts limit to some degree, CT and MRI. Radionuclide studies are extremely useful in the evaluation of joint replacements, especially when infection is suspected. The most widely and often the initial radionuclide test performed is bone scintigraphy. Although sensitive bone scintigraphy is not specific, and it is most useful for screening purposes. A normal study result makes it unlikely that the patient's symptoms are related to the prosthesis. An abnormal study result requires further investigation. The accuracy of bone scintigraphy is between 50% and 70%. Performing the test as a 3-phase study does not improve accuracy (Fig. 9).[37,39-42]

[67]Ga imaging has been used to improve the specificity of bone scintigraphy. [67]Ga, either alone or in combination with bone scintigraphy, has accuracy between 60% and 80% and offers only a modest improvement over bone scintigraphy alone and has fallen into disuse.[37]

Presently, the best available imaging test for diagnosing prosthetic joint infection is WBC marrow imaging with an accuracy of approximately 90% (Fig. 10). All of the studies published over the past 3 decades confirm that this test is highly specific for diagnosing joint replacement infection. In nearly all of the investigations, the test has proved to be sensitive as well.[39,43-48] Its value notwithstanding, as already noted, there are significant disadvantages to the WBC marrow procedure, and investigators continue to search for suitable alternatives.

Boubaker et al[49] reported that ^{99m}Tc-besilesomab was 67% sensitive and 75% specific for diagnosing prosthetic hip infection. When interpreted together with bone scintigraphy, specificity improved to 84%. Gratz et al[50] reported that accuracy improved from 80% for ^{99m}Tc-besilesomab alone to 89% when interpreted in conjunction with bone scintigraphy. Semiquantitative analysis has also been suggested as a way to improve the sensitivity and specificity of ^{99m}Tc-besilesomab for diagnosing lower extremity prosthetic joint infection.[51,52]

Von Rothenburg et al[53] reported a sensitivity of 93% and a specificity of 65% for diagnosing lower extremity prosthetic infection with ^{99m}Tc-sulesomab. Iyengar and Vinjamuri[54] reported similar results. Pakos et al[55] reported that ^{99m}Tc-sulesomab was 75% sensitive, 86% specific, and 79% accurate for diagnosing prosthetic joint infection. Rubello et al[56,57] reported that specificity is improved by imaging at 4 and 20-24 hours after injection. Gratz et al[58] reported that analysis of time activity curves significantly improves the accuracy of ^{99m}Tc-sulesomab for diagnosing moderate and mild prosthetic joint infections.

Although in vivo–labeled leukocytes accumulate in the bone marrow, scant attention has been paid to combining these studies with bone marrow imaging. In one of the few investigations in which bone marrow imaging was performed, Sousa et al[59] reported that, by performing complementary

bone marrow imaging, the specificity of ^{99m}Tc-sulesomab improved from 20% to 100%.

Data on the value of SPECT-CT in suspected prosthetic joint infection are limited. Filippi and Schillaci[60] compared ^{99m}Tc-WBC imaging with SPECT and SPECT-CT in 13 patients with prosthetic joints. Planar imaging correctly identified all 8 infected and all 5 uninfected prostheses (100% accuracy); SPECT-CT provided additional important information by precisely localizing foci of WBC accumulation and facilitating the differentiation of soft tissue from bone infection.

One group evaluated septic loosening of hip prostheses with ^{99m}Tc-sulesomab and reported that SPECT-CT corroborated the antigranulocyte scintigraphy results in 3 patients.[61] In another investigation, 31 patients with 9 infected lower extremity prosthetic joints underwent planar and SPECT-CT imaging with ^{99m}Tc-besilesomab.[62] Sensitivity, specificity, and accuracy for planar imaging alone were 66%, 60%, and 61%, respectively. When planar images were interpreted together with SPECT-CT, sensitivity was unchanged, although specificity and accuracy increased to 73% and 77%, respectively. Even though SPECT-CT improved results, the test was still considerably less accurate than planar WBC marrow imaging.

The potential of SPECT-CT extends well beyond diagnosing infection. In patients with a positive study result, for example, the examination could provide information about the extent of infection (Figs. 10 and 11). Joint aspiration and culture could be performed at the same time. The test also could provide information about other causes of prosthetic failure. Patients might avoid the need to undergo multiple imaging tests at different times and possibly different locations, and a diagnosis could be made more expeditiously.

Diagnosing prosthetic joint infection with ^{18}F-FDG-PET has been investigated extensively. In an early investigation of 74 prosthetic joints, 21 of which were infected, Zhuang et al[63] reported that increased ^{18}F-FDG activity along the bone-prosthesis interface had sensitivity, specificity, and accuracy of 90%, 89.3%, and 89.5%, respectively, for diagnosing prosthetic hip infection and sensitivity, specificity, and accuracy of 90.9%, 72%, and 77.8%, respectively, for diagnosing prosthetic knee infection. Test accuracy depended on location, not intensity, of ^{18}F-FDG uptake. Chacko et al[64] reviewed

^{111}In-WBC   ^{99m}Tc-Sulfur Colloid
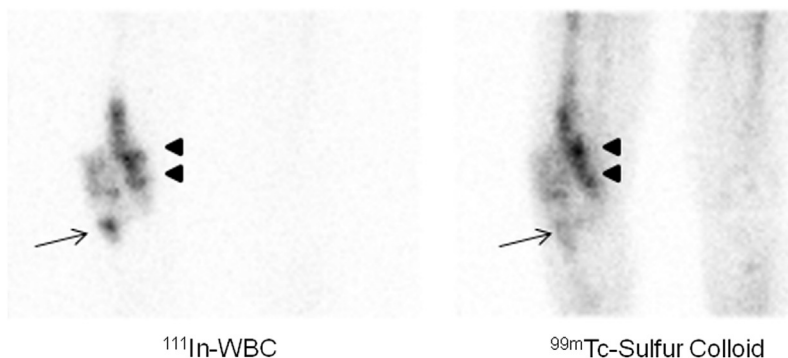
Figure 10 Infected right knee arthroplasty. There is spatially incongruent distribution of activity in the lower lateral aspect of the prosthesis (arrows) on the ^{111}In-WBC (left) and marrow (right) images. There is a more subtle area of incongruence along the upper medial aspect of the prosthesis (arrowheads).
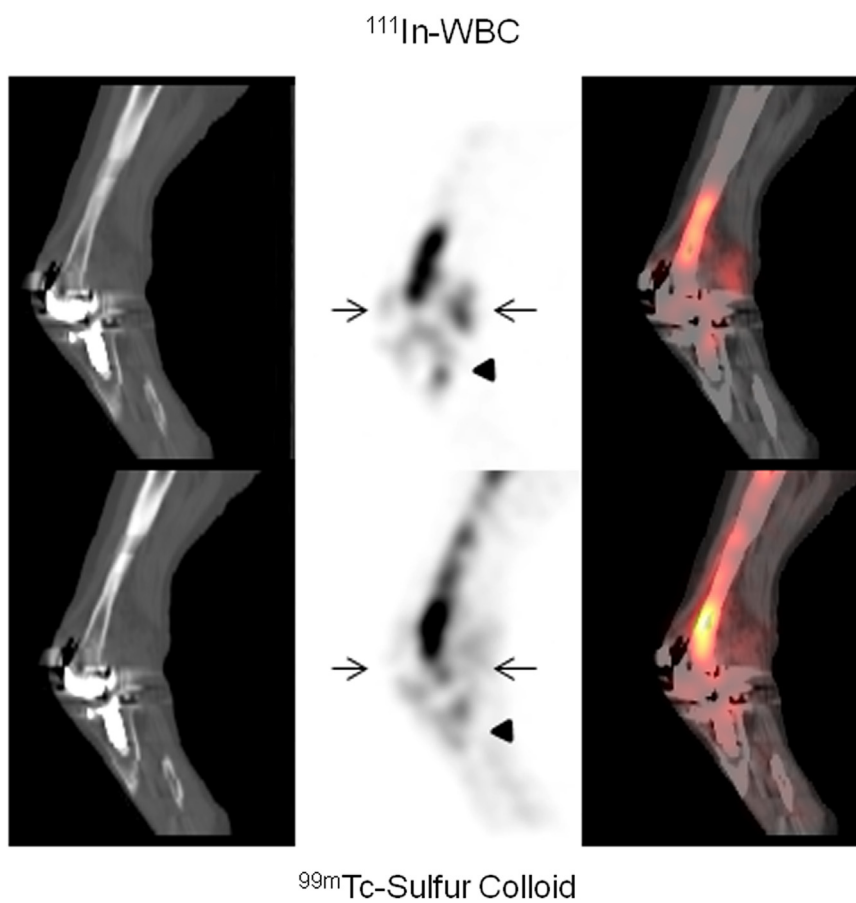
Figure 11 Infected right knee arthroplasty. On the sagittal images from the simultaneously acquired dual-isotope SPECT-CT, spatially incongruent distribution of activity on ^{111}In-WBC (top) and marrow (bottom) images can be identified clearly anterior and posterior to the femoral component (arrows) and posterior to the tibial component (arrowheads). (Same patient as illustrated in Fig. 10.)

^{18}F-FDG-PET scans performed on 89 lower extremity joint replacements. The sensitivity, specificity, and accuracy of the test were 91%, 98%, and 96% respectively, for diagnosing prosthetic hip infection and 92%, 75%, and 81%, respectively, for diagnosing prosthetic knee infection. Test accuracy depended on location and not on intensity of ^{18}F-FDG uptake. Chacko et al[65] in an investigation of 41 painful hip arthroplasties, reported that bone-prosthesis interface activity along the shaft of the femoral component was 92% sensitive and 97% specific for infection and that accuracy depended on location, not intensity, of ^{18}F-FDG uptake.

Reinartz et al[42] studied 92 hip prostheses with 3-phase bone scintigraphy and ^{18}F-FDG-PET. Sensitivity, specificity, and accuracy of 3-phase bone scintigraphy were 68%, 76%, and 74% vs 94%, 95%, and 95%, respectively, for ^{18}F-FDG-PET. They observed that, on ^{18}F-FDG-PET images, activity around the acetabular component and proximal aspect of the femoral component was not associated with infection and that periprosthetic uptake patterns were useful for differentiating infection from aseptic loosening but intensity of uptake was not. Cremerius et al[66] studied 18 patients with painful hip replacements and reported that ^{18}F-FDG-PET was 89% accurate for diagnosing infection. Gravius et al[67] studied 20 patients with painful knee prostheses. The sensitivity and specificity of ^{18}F-FDG-PET

for diagnosing infection were 89% and 82%, respectively. Pill et al[48] studied 92 painful hip prostheses, 21 of which were infected, and reported that ^{18}F-FDG-PET was 95% sensitive and 93% specific for diagnosing infection. A total of 51 prostheses, including 10 infected devices, also were studied with WBC-marrow imaging. The sensitivity and specificity of WBC-marrow imaging in this subgroup were 50% and 95.1%, respectively.

Manthey et al[68] studied 28 lower extremity prostheses and reported that ^{18}F-FDG-PET was 96% accurate for diagnosing prosthetic joint infection. They also reported that by analyzing both intensity and patterns of periprosthetic uptake, it was possible to accurately differentiate aseptic loosening, synovitis, and infection and that activity around the femoral head and neck indicated synovitis plus infection, observations that contradict those of other investigations.[63,65]

Stumpe et al[69] compared bone-prosthesis interface activity to urinary bladder activity in 35 painful hip prostheses. Studies in which periprosthetic activity was intense were classified as positive for infection. ^{18}F-FDG-PET was reasonably specific (81% for reader 1 and 85% for reader 2) but not sensitive (33% for reader 1 and 56% for reader 2) for diagnosing infection (33% for reader 1 and 56% for reader 2). The accuracy of the test for both readers was 69%. Bone scintigraphy was more accurate than ^{18}F-FDG-PET (80% vs 69%).

Van Acker et al[70] studied 21 patients with suspected prosthetic knee infection. ^{18}F-FDG-PET was 100% sensitive but only 73% specific for diagnosing infection. In the same population, [99m]TcWBC-bone imaging was 100% sensitive and 93% specific. Vanquickenborne et al[71] reported that ^{18}F-FDG-PET and ^{99m}Tc-WBC-bone imaging both were 88% sensitive for diagnosing the infected hip replacement. Specificity of ^{18}F-FDG-PET was 78% vs 100% for ^{99m}Tc-WBC-bone imaging.

García-Barrecheguren et al[72] studied 24 hip replacements and reported that ^{18}F-FDG-PET was neither sensitive (64%) nor specific (67%) for infection. Delank et al[73] studied 27 patients with failed lower extremity joint replacements and reported that the test could not reliably differentiate infection from aseptic inflammation.

Love et al[46] evaluated 59 failed lower extremity joint prostheses with ^{18}F-FDG-PET and [111]InWBC-marrow imaging. Among several different criteria used for image interpretation, the presence of bone-prosthesis interface activity, with a target to background ratio greater than 3.6 for hip replacements and 3.1 for knee replacements, was the most accurate (71%) for diagnosing infection. The accuracy of ^{111}In-WBC marrow imaging was 95%. Presently, ^{18}F-FDG imaging does not appear to have a role in the diagnosis of the infected joint replacement.

In view of the similarities in presentation between the inflamed, aseptically loosened prosthesis, and the infected prosthesis and the dramatic differences in their management, the development of an infection-specific imaging agent would be a welcome improvement over current procedures.

^{99m}Tc-UBI 29-41, a radiolabeled synthetic fragment of the naturally occurring human antimicrobial peptide UBI, appears to be able to differentiate between infection and sterile inflammation.[5] In an animal model of prosthetic joint infection, all 6 infected devices studied were positive on day 9.[74] Aryana et al[75] studied 34 painful hip prostheses, 10 of which were infected. The authors interpreted images obtained 30 minutes after injection and reported that the test was 100% accurate.

Diabetic Foot Infection

Diabetic patients can have a significant foot infection without pain and not mount a systemic inflammatory response, and the diagnosis of osteomyelitis often is overlooked. Imaging studies are therefore an essential part of the diagnostic evaluation of these individuals. WBC imaging is considered the radionuclide "gold standard" for diagnosing pedal osteomyelitis in diabetic patients. The sensitivity of planar imaging, using ^{111}In-WBC, has ranged from 72%-100% and the specificity from 67%-100%. The sensitivity and specificity of ^{99m}Tc-WBC planar imaging for diagnosing diabetic pedal osteomyelitis have ranged from 86%-93% and from 80%-98%, respectively.[76] The accuracy of WBC imaging is limited by poor image resolution and the small size of the structure being evaluated, and several investigators have used SPECT-CT in an effort to improve the results.

Heiba et al[77] investigated dual-isotope SPECT-CT using ^{111}In-WBC, bone scintigraphy, and when necessary, bone marrow imaging for diagnosing pedal osteomyelitis in diabetic patients. A total of 213 patients, including 38 with osteomyelitis, were included in their investigation. Simultaneous dual-isotope (^{111}In-WBC + ^{99m}Tc-MDP) SPECT-CT was significantly more accurate than both planar imaging and single-isotope (bone or ^{111}In-WBC) SPECT-CT. Because of the poor resolution inherent in ^{111}In-WBC imaging and the small structures being evaluated, it was not always possible, even with the CT component of the examination, to distinguish between soft tissue and bone infection. The addition of bone SPECT-CT permitted precise localization of WBC accumulation, improving both accuracy and confidence of diagnosis. In another investigation, dual-isotope SPECT-CT was more accurate than conventional imaging for diagnosing and localizing infection in diabetic patients. This technique provided guidance on patient treatment and was associated
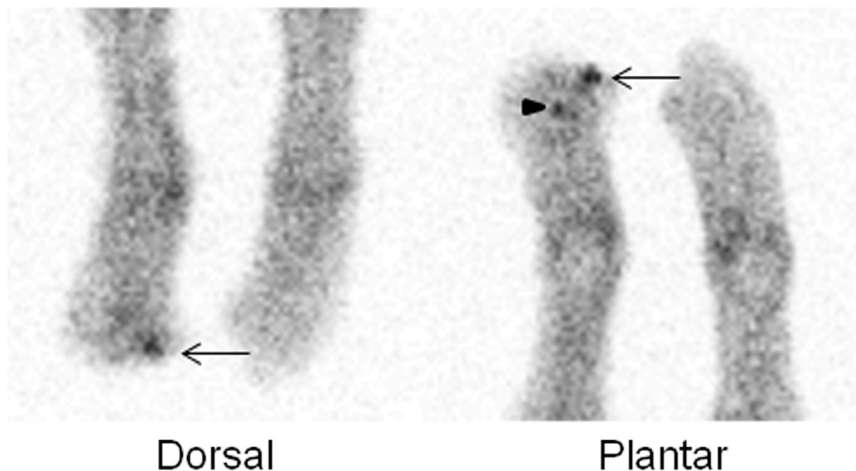
Figure 12 Osteomyelitic right great toe. There is focally increased ^{99m}Tc-labeled leukocyte activity in the right great toe on the dorsal and plantar images (arrows). There is a second focus of increased activity, medial and proximal to this, which is seen only on the planar image (arrowhead). Imaging was performed about 6 hours after ^{99m}Tc-WBC injection.

Figure 13 Osteomyelitis right great toe. SPECT-CT confirms that the great toe focus involves the bone.

with shorter length of hospitalization compared with conventional imaging.[78]

An alternative to dual-isotope SPECT-CT is to use ^{99m}Tc-WBC rather than ^{111}In-WBC. ^{99m}Tc-WBC image resolution is superior, and both labeling and imaging can be performed on the same day. Filippi et al[79] performed ^{99m}Tc-WBC SPECT-CT on 17 diabetic patients with 19 clinically suspected sites of infection. Planar imaging was performed at 30 minutes and at 4 and 24 hours. SPECT-CT was performed at 6 hours. SPECT-CT changed the study interpretation in 10 (53%) sites by excluding osteomyelitis in 6 cases, identifying osteomyelitis in 1 site, and better defining the extent of the infection in 3 sites (Figs. 12-14).

Erdman et al[80] developed a standardized scoring system, the Composite Severity Index (CSI), based on ^{99m}Tc-WBC SPECT-CT. CSI scores were correlated with the probability of favorable outcome during a follow-up period of nearly 1 year. These investigators found that the likelihood of a favorable outcome varied inversely with the CSI score. The CSI score was more accurate at predicting outcome than simply classifying study results as positive or negative for osteomyelitis.

Although ^{67}Ga imaging has been used infrequently in the evaluation of diabetic foot infections, recent data suggest a possible role for ^{67}Ga SPECT-CT in this population. In an investigation of 55 diabetic patients with uninfected pedal

ulcers, Aslangul et al[81] reported that ^{67}Ga SPECT-CT was 88% sensitive and 93.6% specific for diagnosing pedal osteomyelitis.

The role of ^{18}F-FDG-PET and PET-CT in the evaluation of diabetic foot infections has been investigated by several groups. Hopfner et al[82] reported that, in diabetic patients, ^{18}F-FDG-PET correctly identified 95% (37/39) of neuropathic lesions, including 22 of 24 bone lesions and all 15 extraosseous lesions. Sensitivity was not affected by blood glucose levels. Even though none of the subjects had osteomyelitis, the investigators suggested that, because of the relatively low SUV_{max} in the uninfected neuropathic joints, and because of the high SUV_{max} expected in osteomyelitis, ^{18}F-FDG-PET could differentiate osteomyelitis from neuropathic disease.

Basu et al[83] reported that the mean SUV_{max} in uninfected neuropathic joints was 1.3 ± 0.4. The mean SUV_{max} in pedal osteomyelitis was 4.38 ± 1.39, and the SUV_{max} in the 1 case of osteomyelitis superimposed on a neuropathic joint was 6.5. The sensitivity and accuracy of FDG-PET for diagnosing osteomyelitis in this investigation were 100% and 94%, respectively.

Nawaz et al[84] prospectively investigated 110 diabetic patients. Blood glucose level was less than 200 mg/dL in all patients. No information about the presence of foot ulcers was provided. Using visual image analysis only, they reported that ^{18}F-FDG-PET had sensitivity, specificity, and accuracy

Figure 14 Soft tissue infection. SPECT-CT confirms that the focus seen only the planar plantar image is confined to the soft tissues and does not extend into the bone.

of 81%, 93%, and 90% respectively, for diagnosing pedal osteomyelitis.

Schwegler et al[85] prospectively evaluated ^{18}F-FDG-PET for diagnosing clinically unsuspected osteomyelitis in 20 diabetic patients with pedal ulcers. Information on blood glucose levels at the time of imaging was not provided. Only visual image analysis was performed. ^{18}F-FDG-PET detected only 2 (29% sensitivity) of 7 cases of osteomyelitis.

Keidar et al[86] compared ^{18}F-FDG-PET and PET-CT in 18 clinically suspected sites of infection. The accuracy of ^{18}F-FDG-PET-CT for diagnosing pedal osteomyelitis was approximately 94%. The mean SUV_{max} in infection was 5.7 and ranged from 1.7-11.1 for both osseous and soft tissue foci of infection. There was no relationship between the patients' glycemic state and degree of ^{18}F-FDG uptake.

Kagna et al[87] investigated ^{18}F-FDG-PET-CT in 39 diabetic patients (46 sites), 14 of whom had been included in the publication of Keidar et al.[86] Sensitivity, specificity, and accuracy for diagnosing osteomyelitis was 100%, 93%, and 96%, respectively.

Familiari et al[88] compared ^{18}F-FDG-PET-CT with planar Tc-WBC imaging in 13 diabetic patients with a high pretest likelihood of pedal osteomyelitis. All patients had a blood glucose level of less than 160 mg/dL. ^{18}F-FDG-PET-CT imaging was performed at 10 minutes and 1 and 2 hours after injection. The highest accuracy for ^{18}F-FDG-PET-CT at 54% was achieved when the SUV_{max} was ≥ 2.0 at 1 and 2 hours after injection and increased over time. Accuracy improved to 62% when CT findings were taken into account. The accuracy of planar ^{99m}Tc-WBC imaging, in contrast, was 92%.

Presently, the role of ^{18}F-FDG imaging in the workup of diabetic foot requires further investigation.

References

1. Osman DR: Diagnosis and management of musculoskeletal infection. In: Fitzgerald RH, Haufer H, Malkani RL, (eds): Orthopedics. St. Louis: Mosby; 2002. pp. 695-707

2. Palestro CJ, Love C: Radionuclide imaging of musculoskeletal infection: Conventional agents. Semin Musculoskelet Radiol 2007;11:335-352

3. Palestro CJ, Love C, Bhargava KK: Labeled leukocyte imaging: Current status and future directions. Q J Nucl Med Mol Imaging 2009;53:105-123

4. Palestro CJ, Love C, Tronco GG, et al: Combined labeled leukocyte and technetium-99m sulfur colloid marrow imaging for diagnosing musculoskeletal infection: Principles, technique, interpretation, indications and limitations. Radiographics 2006;26:859-870

5. Palestro CJ, Glaudemans AWJM, R.A.J.O. Dierckx: Multiagent imaging of inflammation and infection. Clin Transl Imaging 2013;1:385-396

6. Palestro CJ: FDG-PET in musculoskeletal infections. Semin Nucl Med 2013;43:367-376

7. Forstrom LA, Dunn WL, Mullan BP: Biodistribution and dosimetry of [F-18] fluorodeoxyglucose labeled leukocytes in normal human subjects. Nucl Med Commun 2002;23:721-725

8. Dumarey N, Egrise D, Blocklet D, et al: Imaging infection with ^{18}F-FDG labeled leukocyte PET/CT: Initial experience in 21 patients. J Nucl Med 2006;47:625-632

9. Rini JN, Bhargava KK, Tronco GG, et al: PET with FDG-labeled leukocytes versus scintigraphy with ^{111}In-oxine-labeled leukocytes for detection of infection. Radiology 2006;238:978-987

10. Aksoy SY, Asa S, Ozhan M, et al: FDG and FDG-labelled leucocyte PET/CT in the imaging of prosthetic joint infection. Eur J Nucl Med Mol Imaging 2014;41:556-564

11. Bhargava KK, Gupta RK, Nichols KJ, et al: In-vitro human leukocyte labeling with ^{64}Cu: An intraindividual comparison with ^{111}In-oxine and ^{18}F-FDG. Nucl Med Biol 2009;36:545-549

12. Kumar V, Boddeti DK, Evans SG, et al: Potential use of ^{68}Ga-apo-transferrin as a PET imaging agent for detecting *Staphylococcus aureus* infection. Nucl Med Biol 2011;38:393-398

13. Diaz LA, Foss CA, Thornton K, et al: Imaging of musculoskeletal bacterial infections by [^{124}I]FIAU-PET/CT. PLoS One 2007;10:e1007

14. Love C, Patel M, Lonner BS, et al: Diagnosing spinal osteomyelitis: A comparison of bone and gallium scintigraphy and magnetic resonance imaging. Clin Nucl Med 2002;25:963-977

15. Palestro CJ, Love C, Miller TT: Imaging of musculoskeletal infections. Best Pract Res Clin Rheumatol 2006;20:1197-1218

16. Gemmel F, Dumarey N, Palestro CJ: Radionuclide imaging of spinal infections. Eur J Nucl Med Mol Imaging 2006;33:1226-1237

17. Lievano P, De la Cueva L, Navarro P, et al: ^{67}Ga SPECT/low-dose CT. A case report of spondylodiscitis and Schmorl's node. Rev Esp Med Nucl 2009;28:288-290

18. Domínguez ML, Lorente R, Rayo JI, et al: SPECT-CT with (67)Ga-citrate in the management of spondylodiscitis. Rev Esp Med Nucl Imagen Mol 2012;31:34-39

19. Fuster D, Solà O, Soriano A, et al: A prospective study comparing whole-body FDG PET/CT to combined planar bone scan with ^{67}Ga SPECT/CT in the diagnosis of spondylodiskitis. Clin Nucl Med 2012; 37:827-832

20. Lazzeri E, Pauwels EKJ, Erba P, et al: Clinical feasibility of two-step streptavidin/^{111}In-biotin scintigraphy in patients with suspected vertebral osteomyelitis. Eur J Nucl Med Mol Imaging 2004;31:1505-1511

21. Lazzeri E, Erba P, Perri M, et al: Clinical impact of SPECT/CT with In-111 biotin on the management of patients with suspected spine infection. Clin Nucl Med 2010;35:12-17

22. Guhlmann A, Brecht-Krauss D, Suger G, et al: Chronic osteomyelitis: Detection with FDG PET and correlation with histopathologic findings. Radiology 1998;206:749-754

23. Guhlmann A, Brecht-Krauss D, Suger G, et al: Fluorine-18-FDG PET and technetium-99m antigranulocyte antibody scintigraphy in chronic osteomyelitis. J Nucl Med 1998;39:2145-2152

24. Schiesser M, Stumpe KD, Trentz O, et al: Detection of metallic implant-associated infections with FDG PET in patients with trauma: Correlation with microbiologic results. Radiology 2003;226:391-398

25. Kalicke T, Schmitz A, Risse JH, et al: Fluorine-18 fluorodeoxyglucose PET in infectious bone diseases: Results of histologically confirmed cases. Eur J Nucl Med Mol Imaging 2000;27:524-528

26. Schmitz A, Risse JH, Grunwald F, et al: Fluorine-18 fluorodeoxyglucose positron emission tomography findings in spondylodiscitis: Preliminary results. Eur Spine J 2001;10:534-539

27. Meller J, Koster G, Liersch T, et al: Chronic bacterial osteomyelitis: Prospective comparison of F-18-FDG imaging with a dual-head coincidence camera and In-111-labelled autologous leucocyte scintigraphy. Eur J Nucl Med Mol Imaging 2002;29:53-60

28. Hartmann A, Eid K, Dora C, et al: Diagnostic value of ^{18}F-FDG PET/CT in trauma patients with suspected chronic osteomyelitis. Eur J Nucl Med Mol Imaging 2007;34:704-714

29. Gratz S, Dorner J, Fischer U, et al: F-18-FDG hybrid PET in patients with suspected spondylitis. Eur J Nucl Med Mol Imaging 2002;29: 516-524

30. Ohtori S, Suzuki M, Koshi T, et al: ^{18}F-fluorodeoxyglucose-PET for patients with suspected spondylitis showing Modic change. Spine 2010;15(35):E1599-E1603

31. Stumpe KD, Zanetti M, Weishaupt D, et al: FDG positron emission tomography for differentiation of degenerative and infectious endplate abnormalities in the lumbar spine detected on MR imaging. Am J Roentgenol 2002;179:1151-1157

32. Seifen T, Rettenbacher L, Thaler C, et al: Prolonged back pain attributed to suspected spondylodiscitis. The value of ^{18}F-FDG PET/CT imaging in the diagnostic work-up of patients. Nuklearmedizin 2012;51:194-200

33. Rosen RS, Fayad L, Wahl RL: Increased ^{18}F-FDG uptake in degenerative disease of the spine: Characterization with ^{18}FFDG PET/CT. J Nucl Med 2006;47:1274-1280

34. de Winter F, Gemmel F, Van de Wiele C, et al: 18-Fluorine fluorodeoxyglucose positron emission tomography for the diagnosis of infection in the postoperative spine. Spine 2003;28:1314-1319

35. Nanni C, Errani C, Boriani L, et al: ^{68}Ga-Citrate PET/CT for evaluating patients with infections of the bone: Preliminary results. J Nucl Med 2010;51:1932-1936

36. De Winter F, van de Wiele C, Vogelaers D, et al: Fluorine-18 fluorodeoxyglucose positron emission tomography: A highly accurate imaging modality for the diagnosis of chronic musculoskeletal infections. J Bone Joint Surg Am 2001;83-A:651-660

37. Love C, Marwin SE, Palestro CJ: Nuclear medicine and the infected joint replacement. Semin Nucl Med 2009;39:66-78

38. Tomas X, Bori G, Garcia S, et al: Accuracy of CT-guided joint aspiration in patients with suspected infection status post-total hip arthroplasty. Skeletal Radiol 2011;40:57-64

39. Palestro CJ, Swyer AJ, Kim CK, et al: Infected knee prostheses: Diagnosis with In-111 leukocyte, Tc-99m sulfur colloid, and Tc-99m MDP imaging. Radiology 1991;179:645-648

40. Magnuson JE, Brown ML, Hauser MF, et al: In-111 labeled leukocyte scintigraphy in suspected orthopedic prosthesis infection: Comparison with other imaging modalities. Radiology 1988;168:235-239

41. Levitsky KA, Hozack WJ, Balderston RA, et al: Evaluation of the painful prosthetic joint. Relative value of bone scan, sedimentation rate, and joint aspiration. J Arthroplasty 1991;6:237-244

42. Reinartz P, Mumme T, Hermanns B, et al: Radionuclide imaging of the painful hip arthroplasty: Positron-emission tomography versus triple-phase bone scanning. J Bone Joint Surg Br 2005;87-B:465-470

43. Mulamba L, Ferrant A, Leners N, et al: Indium-111 leucocyte scanning in the evaluation of painful hip arthroplasty. Acta Orthop Scand 1983;54:695-697

44. Palestro CJ, Kim CK, Swyer AJ, et al: Total hip arthroplasty: Periprosthetic indium-111-labeled leukocyte activity and complementary technetium-99m-sulfur colloid imaging in suspected infection. J Nucl Med 1990;31:1950-1955

45. Joseph TN, Mujitaba M, Chen AL, et al: Efficacy of combined technetium-99m sulfur colloid/indium-111 leukocyte scans to detect infected total hip and knee arthroplasties. J Arthroplasty 2001;16:753-758

46. Love C, Marwin SE, Tomas MB, et al: Diagnosing infection in the failed joint replacement: A comparison of coincidence detection fluorine-18 FDG and indium-111-labeled leukocyte/technetium-99m-sulfur colloid marrow imaging. J Nucl Med 2004;45:1864-1871

47. El Espera I, Blondet C, Moullart V, et al: The usefulness of ^{99m}Tc sulfur colloid bone marrow scintigraphy combined with ^{111}In leucocyte scintigraphy in prosthetic joint infection. Nucl Med Commun 2004;25:171-175

48. Pill SG, Parvizi J, Tang PH, et al: Comparison of fluorodeoxyglucose positron emission tomography and (111)indium-white blood cell imaging in the diagnosis of periprosthetic infection of the hip. J Arthroplasty 2006;21:91-97

49. Boubaker A, Delaloye AB, Blanc CH, et al: Immunoscintigraphy with antigranulocyte monoclonal antibodies for the diagnosis of septic loosening of hip prostheses. Eur J Nucl Med 1995;22:139-147

50. Gratz S, Höffken H, Kaiser JW: Nuclear medical imaging in case of painful knee arthroplasty. Radiologe 2009;49:59-67

51. Klett R, Steiner D, Puille M, et al: Antigranulocyte scintigraphy of septic loosening of hip endoprosthesis: Effect of different methods of analysis. Nuklearmedizin 2001;40:75-79

52. Klett R, Kordelle J, Stahl U, et al: Immunoscintigraphy of septic loosening of knee endoprosthesis: A retrospective evaluation of the antigranulocyte antibody BW 250/183. Eur J Nucl Med Mol Imaging 2003;30:1463-1466

53. Von Rothenburg T, Schoellhammer M, Schaffstein J, et al: Imaging of infected total arthroplasty with Tc-99m-labeled antigranulocyte antibody Fab' fragments. Clin Nucl Med 2004;29:548-551

54. Iyengar KP, Vinjamuri S: Role of [99m]Tc Sulesomab in the diagnosis of prosthetic joint infections. Nucl Med Commun 2005;26:489-496

55. Pakos EE, Fotopoulos AD, Stafilas KS, et al: Use of (99m)Tc-sulesomab for the diagnosis of prosthesis infection after total joint arthroplasty. J Int Med Res 2007;35:474-481

56. Rubello D, Casara D, Maran A, et al: Role of anti-granulocyte Fab' fragment antibody scintigraphy (LeukoScan) in evaluating bone infection: Acquisition protocol, interpretation criteria and clinical results. Nucl Med Commun 2004;25:39-47

57. Rubello D, Rampin L, Banti E, et al: Diagnosis of infected total knee arthroplasty with anti-granulocyte scintigraphy: The importance of a dual-time acquisition protocol. Nucl Med Commun 2008;29:331-335

58. Gratz S, Behr TM, Reize P, et al: (99m)Tc-Fab' fragments (sulesomab) for imaging septically loosened total knee arthroplasty. J Int Med Res 2009;37:54-67

59. Sousa R, Massada M, Pereira A, et al: Diagnostic accuracy of combined ^{99m}Tc-sulesomab and ^{99m}Tc-nanocolloid bone marrow imaging in detecting prosthetic joint infection. Nucl Med Commun 2011;32:834-839

60. Filippi L, Schillaci O: Tc-99m HMPAO-labeled leukocyte scintigraphy for bone and joint infections. J Nucl Med 2006;47:1908-1913

61. Kaisidis A, Megas P, Apostolopoulos D, et al: SPECT scan with ^{99m}Tc-labeled monoclonal antibodies. Orthopade 2005;34:462-469

62. Graute V, Feist M, Lehner S, et al: Detection of low-grade prosthetic joint infections using ^{99m}Tc-antigranulocyte SPECT/CT: Initial clinical results. Eur J Nucl Med Mol Imaging 2010;37:1751-1759

63. Zhuang H, Duarte PS, Pourdehnad M, et al: The promising role of ^{18}F-FDG PET in detecting infected lower limb prosthesis implants. J Nucl Med 2001;42:44-48

64. Chacko TK, Zhuang H, Nakhoda KZ, et al: Applications of fluorodeoxyglucose positron emission tomography in the diagnosis of infection. Nucl Med Commun 2003;24:615-624

65. Chacko TK, Zhuang H, Stevenson K, et al: The importance of the location of fluorodeoxyglucose uptake in periprosthetic infection in painful hip prostheses. Nucl Med Commun 2002;23:851-855

66. Cremerius U, Mumme T, Reinartz P, et al: Analysis of (18)F-FDG uptake patterns in PET for diagnosis of septic and aseptic loosening after total hip arthroplasty. Nuklearmedizin 2003;42:234-239

67. Gravius S, Gebhard M, Ackermann D, et al: Analysis of ^{18}F-FDG uptake pattern in PET for diagnosis of aseptic loosening versus prosthesis infection after total knee arthroplasty. A prospective pilot study. Nuklearmedizin 2010;49:115-123

68. Manthey N, Reinhard P, Moog F, et al: The use of [^{18}F] fluorodeoxyglucose positron emission tomography to differentiate between synovitis, loosening and infection of hip and knee prostheses. Nucl Med Commun 2002;23:645-653

69. Stumpe KD, Notzli HP, Zanetti M, et al: FDG PET for differentiation of infection and aseptic loosening in total hip replacements: Comparison with conventional radiography and three-phase bone scintigraphy. Radiology 2004;231:333-341

70. Van Acker F, Nuyts J, Maes A, et al: FDG-PET, ^{99m}Tc-HMPAO white blood cell SPET and bone scintigraphy in the evaluation of painful total knee arthroplasties. Eur J Nucl Med 2001;28:1496-1504

71. Vanquickenborne B, Maes A, Nuyts J, et al: The value of (18)FDG-PET for the detection of infected hip prosthesis. Eur J Nucl Med Mol Imaging 2003;30:705-715

72. García-Barrecheguren E, Rodríguez Fraile M, Toledo Santana G, et al: FDG-PET: A new diagnostic approach in hip prosthetic replacement. Rev Esp Med Nucl 2007;26:208-220

73. Delank KS, Schmidt M, Michael JW, et al: The implications of ^{18}F-FDG PET for the diagnosis of endoprosthetic loosening and infection in hip and knee arthroplasty: Results from a prospective, blinded study. BMC Musculoskelet Disord 2006;7:20

74. Sarda-Mantel L, Saleh-Mghir A, Welling MM, et al: Evaluation of ^{99m}Tc-UBI 29-41 scintigraphy for specific detection of experimental Staphylococcus aureus prosthetic joint infections. Eur J Nucl Med Mol Imaging 2007;34:1302-1309

75. Aryana K, Hootkani A, Sadeghi R, et al: (99m)Tc-labeled ubiquicidin scintigraphy: A promising method in hip prosthesis infection diagnosis. Nuklearmedizin 2012;51:133-139

76. Palestro CJ, Love C: Nuclear medicine and diabetic foot infections. Semin Nucl Med 2009;39:52-65

77. Heiba SI, Kolker D, Mocherla B, et al: The optimized evaluation of diabetic foot infection by dual isotope SPECT/CT imaging protocol. J. Foot Ankle Surg 2010;49:529-536

78. Heiba S, Kolker D, Ong L, et al: Dual-isotope SPECT/CT impact on hospitalized patients with suspected diabetic foot infection: Saving limbs, lives, and resources. Nucl Med Commun 2013;34:877-884

79. Filippi L, Uccioli L, Giurato L, et al: Diabetic foot infection: Usefulness of SPECT/CT for ^{99m}Tc-HMPAO-labeled leukocyte imaging. J Nucl Med 2009;50:1042-1046

80. Erdman WA, Buethe J, Bhore R, et al: Indexing severity of diabetic foot infection with ^{99m}Tc-WBC SPECT/CT hybrid imaging. Diabetes Care 2012;35:1826-1831

81. Aslangul E, M'bemba J, Caillat-Vigneron N, et al: Diagnosing diabetic foot osteomyelitis in patients without signs of soft tissue infection by coupling hybrid ^{67}Ga SPECT/CT with bedside percutaneous bone puncture. Diabetes Care 2013;36:2203-2210

82. Hopfner S, Krolak C, Kessler S, et al: Preoperative imaging of Charcot neuroarthropathy in diabetic patients: Comparison of ring PET, hybrid PET, and magnetic resonance imaging. Foot Ankle Int 2004;25:890-895

83. Basu S, Chryssikos T, Houseni M, et al: Potential role of FDG-PET in the setting of diabetic neuro-osteoarthropathy: Can it differentiate uncomplicated Charcot's neuropathy from osteomyelitis and soft tissue infection? Nucl Med Commun 2007;28:465-472

84. Nawaz A, Torigian DA, Siegelman ES, et al: Diagnostic performance of FDG-PET, MRI, and plain film radiography (PFR) for the diagnosis of osteomyelitis in the diabetic foot. Mol Imaging Biol 2010;12:335-342

85. Schwegler B, Stumpe KD, Weishaupt D, et al: Unsuspected osteomyelitis is frequent in persistent diabetic foot ulcer and better diagnosed by MRI than by ^{18}F-FDG PET or ^{99m}Tc-MOAB. J Intern Med 2008;263:99-106

86. Keidar Z, Militianu D, Melamed E, et al: The diabetic foot: Initial experience with ^{18}F-FDG-PET/CT. J Nucl Med 2005;46:444-449

87. Kagna O, Srour S, Melamed E, et al: FDG PET/CT imaging in the diagnosis of osteomyelitis in the diabetic foot. Eur J Nucl Med Mol Imaging 2012;39:1545-1550

88. Familiari D, Glaudemans AWJM, Vitale V, et al: Can sequential ^{18}F-FDG-PET/CT imaging replace WBC imaging in the diabetic foot? J Nucl Med 2011;52:1012-1019